Polyurethane shape-memory polymers for biomedical applications

9

Y.Q. Fu[1], *W.M. Huang*[2], *J.K. Luo*[3], *H. Lu*[4]
[1]Northumbria University, Newcastle upon Tyne, United Kingdom; [2]Nanyang Technological University, Singapore; [3]University of Bolton, Bolton, United Kingdom; [4]Harbin Institute of Technology, Harbin, China

9.1 Introduction

Polyurethanes (PUs) are a group of polymer materials with long and tangled linear polymer chains showing shape-memory effect (SME) (Kim et al., 1996; Huang et al., 2010b; Leng and Du, 2010). Shape-memory polyurethane (SMPU) is basically composed of soft and hard segments; thermodynamic immiscibility between these two segments leads to phase separation, which makes SMPU an excellent candidate for a shape-memory material (Huang et al., 2010b; Huang et al., 2012). In a relaxed state after fabrication of the SMPU, partially separated soft and hard segments co-exist in the polymer (Lendlein and Kelch, 2002, 2005; Behl and Lendlein, 2007; Huang et al., 2012). Hard segments act as pivot points for shape recovery, whereas soft segments are responsible for absorbing external stress applied on the SMPU. At temperatures below glass transition temperature, T_g, the soft segments do not have enough kinetic energy to achieve good mobility; thus, SMPUs are relatively difficult to be deformed in the glass state. Above T_g, SMPU transforms from a glass state to a rubber state and becomes easily deformed (see Figure 9.1, Yang, 2007). Under an external stress, the soft and hard segments reorient themselves in the direction of external force, becoming stretched (Lendlein and Kelch, 2002; Behl and Lendlein, 2007). By cooling SMPUs below T_g while maintaining the deformed shape with applied force, the mobility of the soft segments is restricted so that the deformation is maintained after removal of the constraints, as shown in Figure 9.1 (Yang, 2007). Upon re-heating above T_g, the soft segments obtain enough mobility to return to their original curled shape, resulting in the shape recovery of the SMPU.

Compared with other types of shape-memory polymers (SMPs), PU-based SMPs have many advantages, including easy processing, low cost of materials and fabrication, large recovery strains up to 1000%, wide, adjustable shape-recovery temperature range, excellent chemical properties, and biocompatibility for most SMPUs (Liang et al., 1997; Wei et al., 1998; Zdrahala and Zdrahala, 1999; Metcalfe et al., 2003; Leng and Du, 2010). The properties of SMPU, such as elasticity, crystallization temperature range, melting point, and thermal and deformation behavior, can be

Shape Memory Polymers for Biomedical Applications. http://dx.doi.org/10.1016/B978-0-85709-698-2.00009-X
© 2015 Elsevier Ltd. All rights reserved.

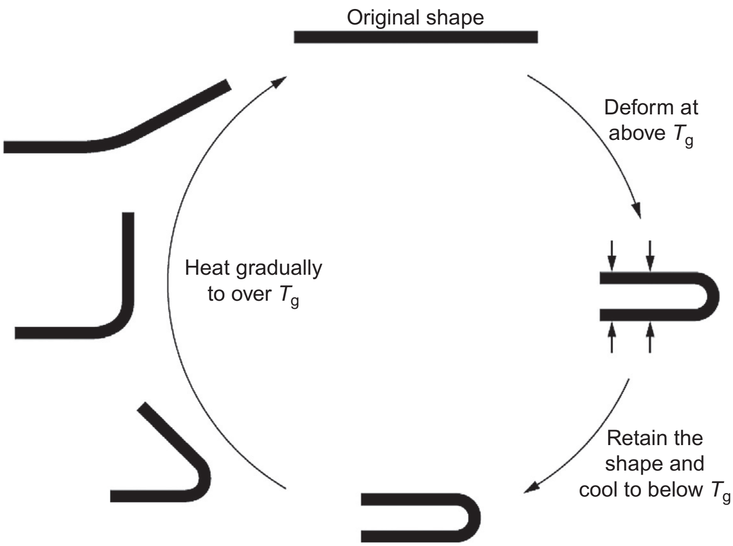

Figure 9.1 Illustration of shape-memory effect (Zhao et al., 2011).

easily tailored by changing the ratio of hard and soft segments (Leng and Du, 2010; Zhao et al., 2011).

Based on the nature of cross-linking, SMPUs can be divided into two main categories (see Figure 9.2) (Monkman, 2000a; Leng and Du, 2010; Huang et al., 2012). The first is physically cross-linked SMPUs, or thermoplastic SMPUs. Thermoplastic SMPUs are flexible and can be reshaped, as their hard segment network structures consist of long sequences of weak bonds (see Figure 9.2a). Due to their flexibility and easy reshaping, thermoplastic SMPUs are the most commonly used SMPUs for many applications (Jeong et al., 2000; Leng and Du, 2010). The second is chemically cross-linked SMPUs, or thermoset SMPUs (see Figure 9.2b), which possess a higher modulus in comparison with thermoplastic SMPUs. They lack thermal plasticity and are difficult to process, thus making them difficult for recycling and reprocessing (Huang et al., 2012).

The polyurethane SMP invented by Hayashi (1990) is currently the most studied polyurethane SMP (Tobushi et al., 1996). Mitsubishi Heavy Industries (MHI) has done extensive research on the SMPU since 1980s (Wei et al., 1998; Merlin, 2008). The T_g values of the MHI SMPUs have a wide temperature range from −30 to 65 °C, which can be applied in many commercial uses, including kitchen tools, textiles, automotive components, biomedical devices, etc. Hu's group has synthesized the SMPUs, which are mainly for textile applications (Hu et al., 2003; Zhuo et al., 2008; Chen et al., 2007a,b; Zhu et al., 2006). Work on the enhancement and triggering mechanisms of the SMPUs PU foam has been proposed and investigated by Sokolowski et al. (2007). Electrospun SMPU nanofibers have also been made (Zhuo et al., 2008). To enhance the strength of polyurethane SMPU, various fillers, such as metals, silica

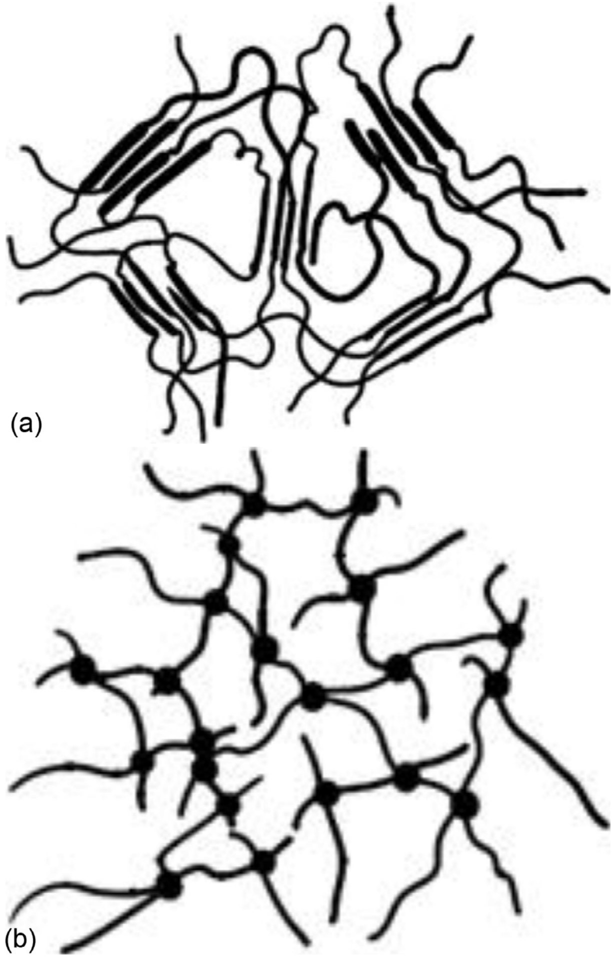

Figure 9.2 Physically (a) and chemically (b) cross-linked SMPUs.

particles, clay, carbon nanofibers (CNFs), carbon nanoparticles (CNPs), carbon nanotubes (CNTs), and graphene, have been added to PU, forming the SMP composites (Gunes et al., 2008; Cao and Jana, 2007). Although the shape recovery of SMPUs is intrinsically a thermally induced process, it can also be triggered optically, electrically, magnetically, or electromagnetically, with the addition of various functional fillers or nanoparticles (Sahoo et al., 2010; Gunes et al., 2009; Cho et al., 2005; Jung and Cho, 2010; Razzaq et al., 2007a,b).

SMPUs have been developed rapidly in recent years for medical device applications because they possess some unique properties: biocompatibility, easy to adjust transition temperatures around human body temperature (Ahmad et al., 2011), low cost, and easy synthesis procedures. Recently, reprocessability and reusability have been studied by Ahmad et al. (2012a). Various shape-memory stimuli methods other than heat, such as water, electric, light, or magnetic actuation, and magnetic field have broadened their potential medical applications significantly (Sokolowski et al., 2007; Huang et al., 2012). Some successful biomedical applications include the vascular stent (Baer et al., 2007), SMP wire for thrombus removal, deployable biomedical devices, SMP wires for suture, etc. (Small et al., 2010).

In this chapter, an overview of the properties of PU will be presented, followed by various shape-memory triggering methods. The medical applications of the SMPUs will be discussed in detail.

9.2 Properties of shape-memory polyurethane (SMPU)

9.2.1 Microstructure

PUs are made of long tangled polymer chains consisting of two segments: flexible, soft segments; and elastic and relatively hard segments. By selecting a proper combination and/or ratio of soft segment to hard segment, various properties such as elasticity, crystallization temperature range, and melting point can be obtained. PUs are generally produced from the reaction of molecules containing two or more isocyanate groups (—NCO) with polyol molecules containing two or more hydroxyl groups (—OH) (Huang et al., 2012). A few examples are shown in Figure 9.3. The most commonly used diisocyanates include 4,4′-diphenylmethane diisocyanate (MDI), phenylene diisocyanate (PDI), toluene diisocyanate, hexamethylene diisocyanate, and isophorone diisocyanate (IPDI) (Szycher, 1999; Bassi et al., 2003). A short chain diol, referred to as a chain extender, is normally used to produce hard segments by reacting with diisocyanate; for example, 1,4 butandiol (Ahmad et al., 2012a). Catalysis also plays an important role in the preparation of SMPUs, since it influences not only the chemical reaction rate but also the chain propagation, extension, and cross-linking (Ahmad et al., 2012a). Some commonly used catalysts include tertiary amines and organometallics. A few key factors influencing the shape-memory behaviors of SMPUs are summarized below.

9.2.1.1 Hard segment structure

Dependence of shape-memory behavior on hard segment content has been extensively studied (Yang et al., 2003). Lee et al. (2001) reported that SMPUs with 20 or 25 wt% of hard segment did not show shape-recovery effect because they did not have strong chemical interaction or physical cross-links due to the low content of hard segments. SMPUs with 50 wt% of hard segment content showed strong interaction among the hard segments, which resulted in a rigid structure and loss of shape-memory behavior. However, 80−95% of shape recovery was obtained for this SMPU with 30−45 wt% of hard segment content. Lowering the content of hard segments increases the hysteresis in shape-memory behavior (Lee et al., 2001, 2004). Therefore, hard segment percentage is critical in the synthesis of high-quality SMPUs. Increase in hard

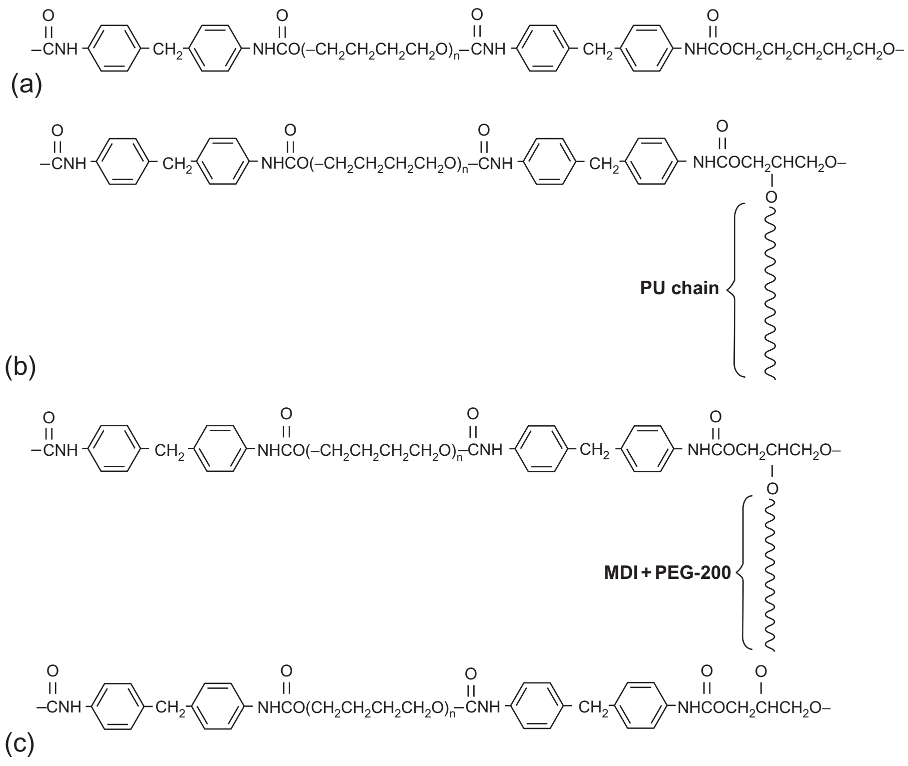

Figure 9.3 Structures of PU SMPs based on PTHF, MDI, PEG, and propanetriol with (a) linear, (b) grafted, and (c) cross-linked structure.

segment content can increase compatibility between the soft and hard segments (Huang et al., 2012). The increase in the glass transition temperature of the SMPU was also observed with the increase of hard segment content, which is attributed to the enhanced hydrogen bonding and rigidity of molecular chains (Ahmad et al., 2012b).

The effect of hard segment on the SMPU structures was studied by Yang et al. (2003). They used two different diisocyanates with different molecular structures: PDI and MDI. PDI has a planar shape, whereas MDI has a non-planar shape. PDI-based SMPUs possess superior mechanical properties over MDI-based SMPUs because of their higher crystallinity (Huang et al., 2012). The SMPUs with the PDI as the hard segment show a better shape-recovery ratio than those with MDI-based SMPUs (Yang et al., 2003). For the synthesis of medical-grade SMPUs, the MDI is often selected because of its low toxicity. Although MDI is most commonly used as the hard segment, IPDI has the advantage of producing polymers with high resistance to UV-light-related degradation, good long-term stability, and high tensile strength (Bassi et al., 2003). Hence, the combination of various diisocyanates is often used to improve the overall properties of SMPUs. For example, MDI was used to synthesis medical-grade SMPUs, while IPDI was introduced to increase the stiffness of SMPUs (Szycher, 1999; Ahmad et al., 2012a).

Addition of small monomer units in the hard segment can enhance thermo-mechanical properties of the SMPUs (Chen et al., 2007b). For example, Ding et al. (2006) found that introducing polyethylene glycol-200 (PEG-200) in hard segment (10–15%) enhanced the mechanical properties of SMPUs. An addition of PEG-200 in the SMPUs can suppress the mobility of soft segments and decrease the crystallinity of polyol and heat of fusion of SMPUs, thus enhancing the compatibility between soft and hard segments (Ding et al., 2006; Merline et al., 2008).

9.2.1.2 Soft segment structure

The long-chain polyol segments in the SMPUs are responsible for the formation of soft domains. At room temperature, the polyols can be liquid or solid, depending on their molecular weight. Long-chain polyol molecules show good flexibility and low transition temperature due to their aliphatic structure and intermolecular interactions, particularly the abundant ether bonds (Ma et al., 1997; Ahmad et al., 2012b). Consequently, the chemical structure of polyols, the reaction between the polyol and diisocyanate, and the degree of phase separation are all important for shape-memory properties of the SMPUs (Ahmad et al., 2012b). Polyols with different structures and reactivities can be used to tailor the thermo-mechanical and shape-memory properties of SMPUs (Goethals et al., 1998). Adding different types of polyols provides the SMPUs with various properties. The polyols are generally divided into two major types: polyether and polyester polyols (Chun et al., 2006). PUs based on polyether polyols are more hydrolysis-resistant than those based on polyester polyols, whereas SMPUs with polytetramethylene ether glycol have good hydrolysis and microbial resistance as well as excellent dynamic properties (Ahmad et al., 2012b). Polycaprolactone polyols have the inherent toughness and resistance of polyester and can improve the low-temperature performance of the SMPUs.

9.2.1.3 Phase separation

SMPUs typically present a micro-phase separated structure due to the thermodynamic incompatibility between the hard segment and soft segment. The micro-phase separation is thus essential for the shape-memory properties as well as for the mechanical performance, as it results in the formation of regions rich in hard segment (domains) that act as cross-linking points for the soft/switching segments (Ahmad et al., 2012b; Chen et al., 2006). Flexibility, strength, and toughness of thermoplastic PUs are dependent on the degree of phase separation of hard and soft segment domains, apart from the structure of polyols, choice of chain extenders, ratio of the hard and soft segment, the reaction process and conditions, etc. (Hu et al., 2003). Phase distribution and separation, phase composition, and micro domain size have a significant impact on the mechanical performance and shape-memory properties of SMPUs.

9.2.2 Thermo-mechanical behavior SMPU

To evaluate the mechanical and thermo-mechanical properties of SMPUs, various methods have commonly applied, including tensile tests, dynamic mechanical/thermal analysis, shape-recovery test, stability tests, etc. (Huang et al., 2006). Uniaxial tensile tests are the mostly frequently used method to investigate the behavior of the polyurethane SMP under uniaxial tension.

9.2.2.1 Stress–strain–temperature relationship

The stress–strain–temperature (σ–δ–T) relationship of SMPUs has been widely studied (Lendlein and Kelch, 2002; Huang et al., 2012). There are four steps for testing the thermo-mechanical properties of the PU-based SMPs (Tobushi et al., 1992, 2001).

(1) At a high temperature T_h ($>T_g$), the SMP specimen is loaded to a pre-determined maximum strain (ε_m) at a constant strain rate.
(2) The SMP sample is held at ε_m and cooled to a low temperature T_l ($<T_g$).
(3) After full unloading, only a very small amount of elastic strain is recovered.
(4) The free-standing sample is heated from T_l to T_h at a constant heating rate. The pre-strain is almost fully recovered with only a very small amount of strain left at T_h.

A typical stress–strain curve of the SMPU at room temperature is illustrated in Figure 9.4a; ε_t, ε_h, and ε_i denote the elastic strain, total instant recovery strain upon unloading, free recovery strain during holding (without any external load), and final residual strain, respectively (Yang, 2007). In the deformation of the SMPU, the maximum strain ε_m can be defined as:

$$\varepsilon_m = \varepsilon_t + \varepsilon_h + \varepsilon_i \tag{9.1}$$

Figure 9.4b presents one example of the strain *vs.* stress relationships of the SMPU upon loading to different maximum strains, ε_m, namely, 20%, 50%, and 100%, followed by unloading to zero stress with a loading strain rate of 10^{-3}/s (Yang et al., 2004, 2005; Yang, 2007). Upon unloading, recovery is largely attributed to elastic recovery, in particular at the early unloading stages in the small maximum strain cases.

Tensile tests were also carried out at four different strain rates at $T_g + 15$ °C following the above procedure, as shown in Figure 9.5 (Yang, 2007; Huang et al., 2012). The residual strain (ε_i) is a very small portion of maximum strain (ε_m) and decreases continuously upon further holding of the loads. Result reveals that a higher strain rate results in more instant recovery strain. It is known that, if loading time is short, the strain energy in a polymer can be stored by quick mechanical deformation at a temperature above T_g. A significant amount of strain may be recovered, but only gradually with the elapse of time. Clearly, the strain recovery is highly dependent on the strain rate. With the increase of strain rate, the elastic strain ε_t becomes smaller while ε_h increases. Since ε_i is mainly ascribed to the viscous flow of a material that is highly dependent on the strain rate, ε_i increases with the strain rate (Huang et al., 2012).

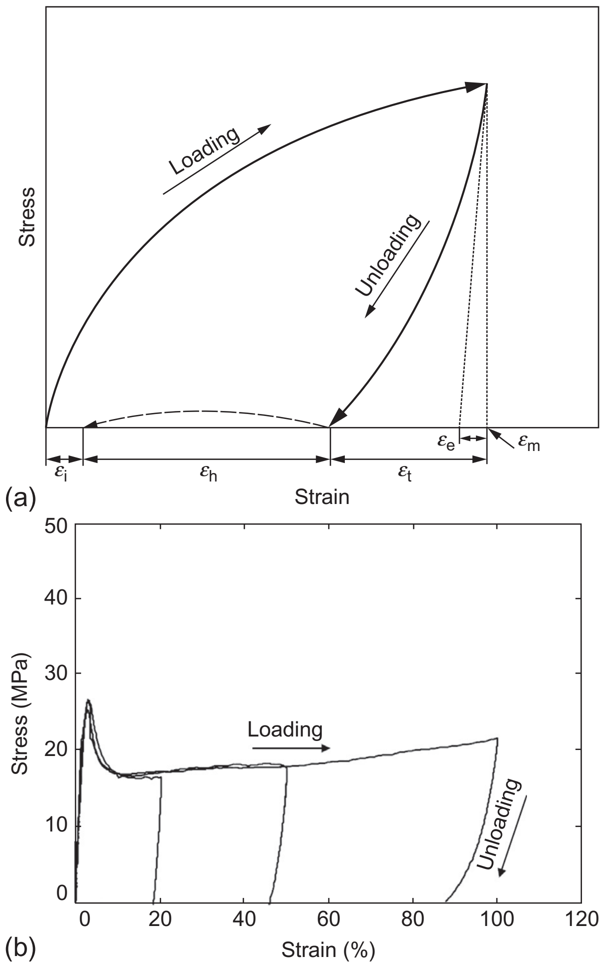

Figure 9.4 (a) Example of loading/unloading uniaxial tensile test; (b) strain versus stress relationships of SMP in loading/unloading to different maximum strains, namely, 20%, 50%, and 100%, followed by unloading to zero stress with a loading rate of 10^{-3} s (Yang et al., 2007).

The dependence of strain recovery upon the maximum pre-strain was investigated using standard tensile tests (Huang et al., 2012). The samples were loaded to different maximum strains and then unloaded to zero stress at a strain rate of 10^{-2}/s and at T_g+5 °C. The maximum pre-strains were from 50% to 600% at a 50% interval; the relationships of stress versus strain are plotted in Figure 9.6 (Yang, 2007; Huang et al., 2012). The SMP samples experienced obvious "creeping" in the strain range from 100% to 300%, followed by hardening due to reorientation and crystallization. Generally speaking, the recovery ratio decreases with the increase of maximum strain, whereas the decrease rate is more significant at a maximum strain above 200% and negligible at a maximum strain range from 100% to 200% (Huang et al., 2012).

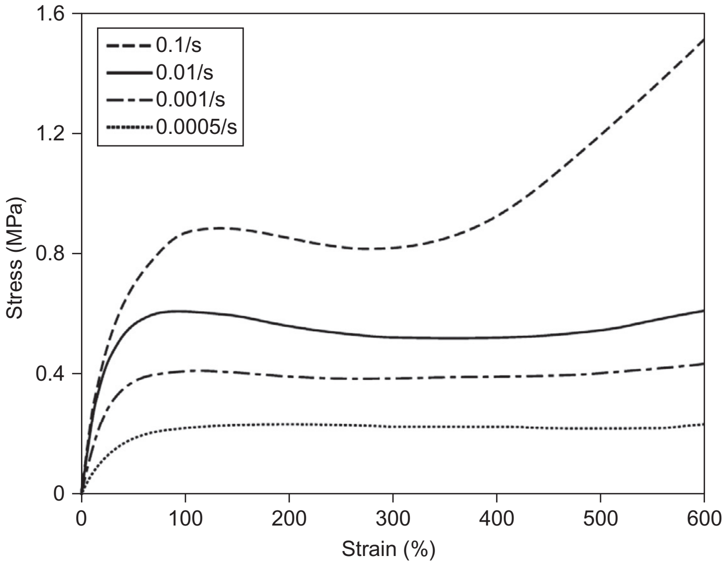

Figure 9.5 Strain-versus-stress relationships of polyurethane SMP MM3520 at $T_g + 15$ °C. From Yang et al. (2007).

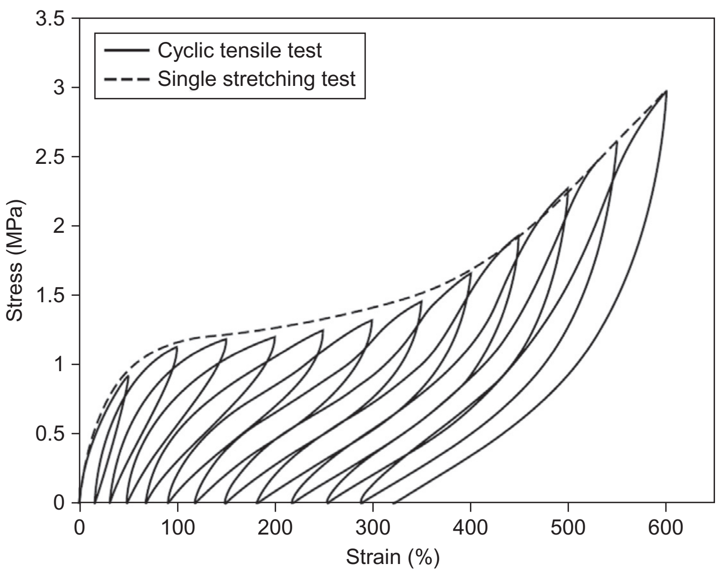

Figure 9.6 Results of cyclic tensile test and single stretching test at a constant strain rate of 0.01^{-1} s at $T_g + 5$ °C.
From Yang (2007).

The decrease in the total instant recovery ratio can be attributed to reorientation and crystallization of the SMPUs, and the sudden decrease in the recovery ratio may be a result of decoupling in the imperfect crystalline part of the polymer in the first a few cycles (Tobushi et al., 1996).

9.2.2.2 Shape recovery tests

Recovery stress and recoverable strain are all essential in engineering applications of the SMPUs. The shape recovery of the SMPUs at different conditions was systematically studied (Huang et al., 2012). The SMPU wires were uniaxially stretched at 50 °C with a 100 N load cell to three different maximum strains, 10%, 20%, and 50%. The wires were then rapidly cooled to room temperature in 3 min with their maximum strain held, followed by unloading to zero stress. Subsequently, the pre-strained wires were heated at a constant rate of 2 °C/min. For all the pre-strained wires in the free recovery test, the recovery ratio (ratio of measured recovery strain to pre-strain; 10%, 20%, or 50%) was applied as a measure of the recovery. Figure 9.7 presents the evolution of the recovery stress and recovery ratio against temperature (Yang, 2007; Huang et al., 2012). In Figure 9.7a, the recovery stress reaches a peak at ~30 °C and then falls continuously upon further heating, in particular, at temperatures over 40 °C. The recovery stress almost vanishes at 60 °C. A larger pre-strain results in a larger recovery stress. Upon heating to 60 °C, the recovery (without constraint) was ~100%, as shown in Figure 9.7b (Yang, 2007; Huang et al., 2012).

The shape recovery ability of the SMPU is highly dependent on strain rate, temperature, and maximum strain (Huang et al., 2012). For a higher strain recovery, a higher strain rate is preferred during loading. Furthermore, it is reported that the SMPU is needed to deform at a temperature ranging from T_g+5 °C to T_g+10 °C for more recoverable strain, especially for a larger recoverable strain rate. Since severe hardening at over 200% strain results in some irreversible strain, the polyurethane SMP should be used at a strain below 200% (Huang et al., 2012). The stability of shape-recovery properties of SMP is also highly dependent on the cycle number. Upon cycling, the total instant recoverable strain deteriorates, and the stress corresponding to the maximum strain decreases (Huang et al., 2012).

9.2.2.3 Multi-shape-memory effect and temperature-memory effect

Traditionally, shape recovery of the SMPUs means its shape changes from a temporary shape directly to the original shape. Under special processing of the SMPUs or some special SMPs, shape recovery can be achieved in a step-by-step manner through one or a few intermediate shapes, which is often called multi-SME (Bellin et al., 2006, 2007; Xie et al., 2009; Pretsch, 2010). For example, by immersing different parts of polyurethane SMP wire into water for different durations, a gradient transition temperature can be achieved because of the significant influence of moisture on the glass transition temperature in the SMPU (Yang et al., 2007; Huang et al., 2005); an example is shown in Figure 9.8. If two types of soft segments inside the

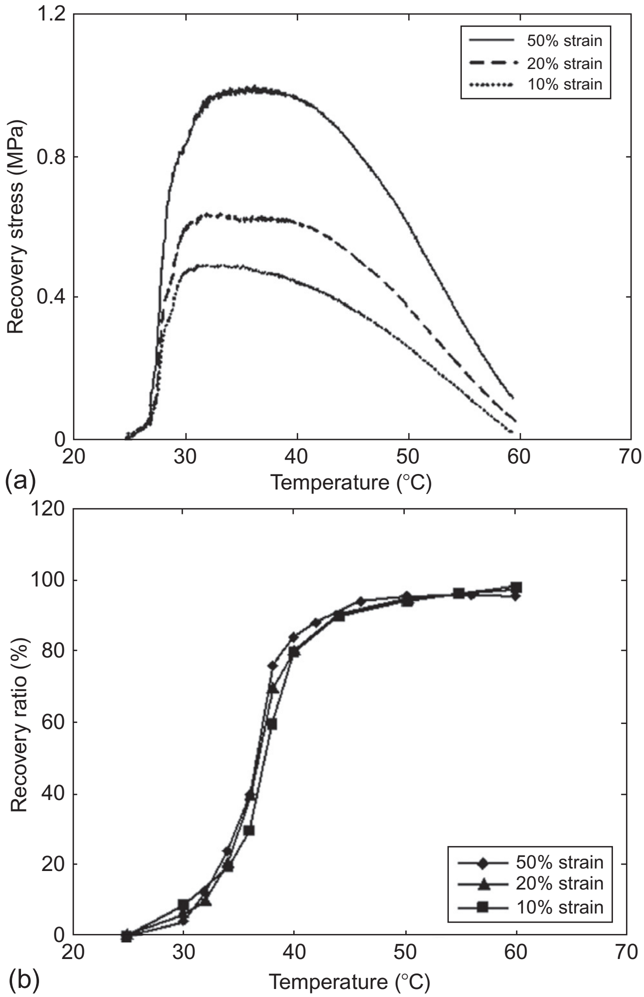

Figure 9.7 Recovery upon heating. (a) Recovery stress as a function of temperature. (b) Shape recovery ratio as a function of temperature.
From Yang (2007).

SMPU are sensitive to different types of stimuli, the triple-SME can be achieved by using different stimuli independently (Behl and Lendlein, 2010; Xie, 2010; Huang et al., 2011). Theoretically, it is possible to use only one soft-segment for the triple-SME by utilizing the glass transition and melting of these two commonly observed transitions in thermoplastic polymers (Huang et al., 2010b). Unlike most metals and their alloys, the multiple SME transition of some polymers occurs over a wide temperature range (Miaudet et al., 2007; Xie, 2010) that serves as a series of sub-transitions to achieve the multi-SME (Xie, 2010).

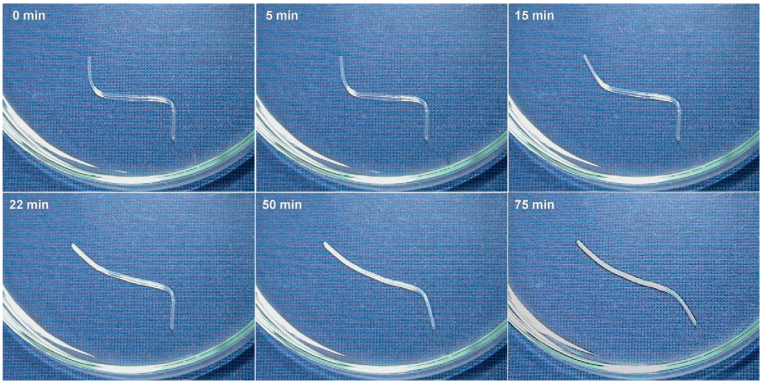

Figure 9.8 The multi-SME in thermo/moisture-responsive PU SMP upon immersing into room temperature water (moisture-responsive).
Reproduced from Huang et al. (2005), with permission.

Temperature memory effect (TME) is another related phenomenon in SMPs occurring during thermal cycling or mechanical cycling (Liu et al., 2005). The previous temperature of interruption is memorized and utilized in a later heating process. Miaudet et al. (2007) reported that in the constrained recovery test of a shape-memory nanocomposite with a broad glass transition temperature range, the maximum recovery stress occurred at the temperature at which the material was pre-deformed to the temporary shape. Huang et al. (2012) systematically studied the TME in SMPs and concluded that the TME is actually not a surprising phenomenon, but a natural response from polymers (Sun and Huang, 2010a,b; Sun et al., 2010).

9.3 Techniques for activating SME

Shape recovery of SMPUs is normally a thermally induced process; however, they can also be triggered optically, electrically, magnetically, or electromagnetically, and so on, with/without adding various functional fillers (Miaudet et al., 2007; Monkman, 2000b; Zhao et al., 2011).

9.3.1 Thermal triggering

The most common method for shape recovery in SMPUs is thermally induced (e.g., Behl and Lendlein, 2007). The SMPUs can be subjected to large deformations at an elevated temperature above their glass transition temperature T_g. Cooling the deformed sample to a temperature below T_g under constraints fixes the deformed shape of the sample. The original shape of the SMPUs will be recovered if the material is heated back to a temperature above T_g without constraints (Xu et al., 2009, 2010; Kim et al., 2010; Huang et al., 2010b).

For SMPU, the SME originates from either a glass transition temperature or melting temperature. Therefore, thermally actuated SMPs must be heated above their characteristic transition temperatures to induce the shape changes. For the SMPUs with transition temperatures close to body temperature, actuation can be accomplished simply by placing the SMP into the body and allowing heat transfer from the adjacent fluid or tissue to induce actuation. However, in some cases, a higher transition temperature would be desired, thus more mechanical rigidity can be maintained in the SMPU (i.e., higher elastic modulus) at body temperature for a precise control of actuation (Leng and Du, 2010).

9.3.2 Electric triggering

SMPU is normally considered as a non-conductive material because of its extremely low electrical conductivity (in the order of 10^{-10}–10^{-15} S/m) (Sahoo et al., 2005). Conductive SMPU can be made by dispersing conductive particles into the non-conductive SMP matrix (Leng et al., 2007; Liu et al., 2009). The fillers used for the conducting SMPs include CNTs (Cho et al., 2005; Paik et al., 2006), CNPs (Yang et al., 2005), conductive fiber (Leng et al., 2007), and metal particles, such as Au or Ni (Schmidt, 2006; Leng et al., 2007, 2008b). At a low concentration of conducting particles, conduction is mainly dominated by hopping conduction among the fillers; thus, its conductivity appears close to those of the bulk PUs, namely insulators (Xu et al., 2010). The SMP composite becomes conductive when the filler concentration is increased to a critical value, or the percolation threshold, which forms the electron bridge within the substrate by the filler and its dispersion state.

Nanosized carbon black (CB) or CNPs have been widely used for electrically conductive nanocomposites (Yang et al., 2005; Leng et al., 2008a; Meng and Hu, 2009; Koerner et al., 2004). The electrical conductivity of shape-memory PU filled with 30% CB is about 1–10^{-1} S/cm (Liu et al., 2009). However, Paik et al. (2006) found that CB is not so effective in improving the mechanical strength and shape-recovery stress of SMPs. Gunes and Jana (2008) prepared PU/CB composites by melt mixing and found that the crystallinity soft segment decreased due to the constraining effect of CBs on the mobility of the soft segment during crystallization. Figure 9.9 shows one example of electric actuation of CNP doped SMPU (Yang, 2007; Huang et al., 2012). The SMP composite was hot-pressed into a plate shape with a thickness of 2.0 mm and then cut into a "n" shape for demonstrating the SME upon heating by passing an electrical current through it. The sample can be easily bent at 60 °C, which is above T_g. Figure 9.9a shows the infrared images of the sample heated by an electrical current for 45 s (Yang, 2007; Huang et al., 2012). After switching off the electrical power and cooling back to 22 °C room temperature with the deformed shape held still, the bent shape was formed. When reheated above T_g by passing an electrical current, the sample recovered its original shape, as shown in Figure 9.9b (Yang, 2007; Huang et al., 2012).

CNFs are not only commonly used for reinforcement applications, but also as electrical conductive fillers as well as catalyst support (Gall et al., 2000, 2004). The temperature and strain have significant influences on the electrical resistivity

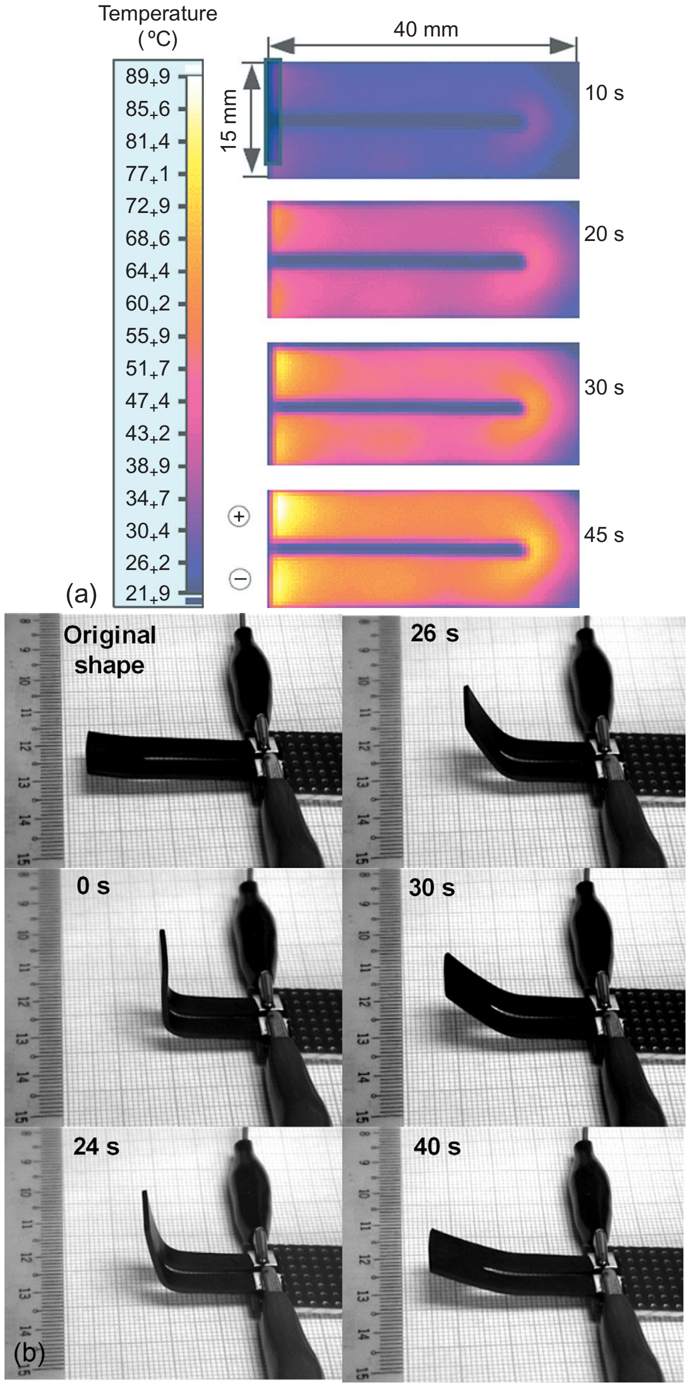

Figure 9.9 Shape-memory effect in conductive SMP carbon nanoparticles. (a) Temperature distribution taken by an infrared camera. (b) Shape-recovery upon passing an electrical current (Yang et al., 2005).

of the CNF-filled SMPs. Gunes et al. (2009) studied the relationship between electrical resistivity and sample temperature of SMPUs filled with CNFs, oxidized-CNFs, and CBs. It was found that CNF- and CB-filled SMPUs showed a positive temperature coefficient of resistivity (Gunes et al., 2009).

CNTs have been extensively studied in recent years as a replacement for the CNPs (Koerner et al., 2004). A SMPU composite incorporating 5 wt% CNTs can have an electrical conductivity of 10^{-3} S/cm (Cho et al., 2005). Paik et al. (2006) prepared PU with CNTs, and the electrical conductivity was about 2.5×10^{-3} S/cm. Because CNTs have tremendously large aspect ratios (100–10,000), many researchers have observed exceptionally low electrical percolation thresholds for CNT-based nanocomposites (Sandler et al., 2003; Bryning et al., 2005). Depending on the matrix, processing technique, and nanotube type, percolation thresholds ranging from 0.001 wt% to more than 10 wt% have been reported (Sandler et al., 2003; Choi et al., 2006). The large dispersion of the percolation threshold for electrical conductive SMPU-CNT nanocomposites is believed to be caused by processing methods used, which may result in different status of disentanglement of CNT agglomerates, uniform spatial distribution of individual CNTs, degree of alignment, dispersion, alignment, aspect ratio, and degree of surface modification of CNTs (Sahoo et al., 2010).

9.3.3 Magnetic triggering

SMPUs doped with ferromagnetic and ferrite particles, such as Ni, or Fe, FeO_x, $MgZnO_x$, and $NiZnFeO_x$, can be inductively heated by magnetic field (Kumar et al., 2010; Small et al., 2009). The electromagnetic energy from the external high frequency electromagnetic field can be transformed to heat if these ferromagnetic particles have been added inside the SMPUs (Spinks et al., 2006; Ahir and Terentjev, 2005; Ahir et al., 2006). Schmidt (2006) and Yakacki et al. (2009) used magnetic fields to remotely actuate SMP composites by incorporating iron (II,III) oxide nanoparticles into thermoplastics and thermoset SMPs (Schmidt, 2006; Razzaq et al., 2007a,b). To improve the particle dispersion in the matrix, the iron (III) oxide nanoparticles were coated with silica (Weigel et al., 2009). By selecting a ferromagnetic particle material with a Curie temperature within a safe medical limit, overheating can be avoided. Selective heating of specific device areas is also possible, and remote actuation can be realized by an externally applied magnetic field (Meng and Hu, 2009; Zhang et al., 2007). Medical devices, such as expandable stents and intravascular microactuators of SMP nanocomposites, have been demonstrated with magnetic field actuation (Buckley et al., 2006).

9.3.4 Water and solution triggering

Shape recovery of the SMPU can be induced by moisture or water that has a significant effect on the glass transition (Haung et al., 2010a; Huang, 2010). When immersed in water, water molecules diffuse into the SMPU samples and act as a plasticizer, leading to the reduction of transition temperature and resulting in shape

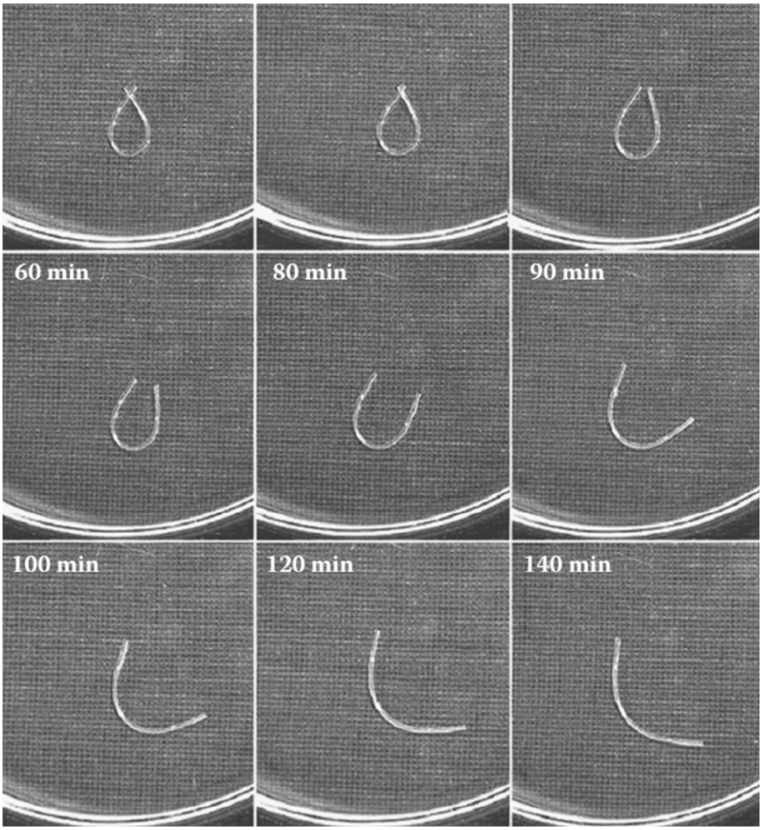

Figure 9.10 Water-driven recovery of an SMPU wire.
Reprinted from Huang et al. (2005), with permission.

recovery, as shown in Figure 9.10 (Huang et al., 2005). In the SMPUs and their composites, T_g is decreased from transition temperature to or below ambient temperature after immersion into water. The decrease of the T_g depends on the moisture uptake, which indirectly depends on the immersion time (Huang et al., 2005; Yang et al., 2004, 2006).

The SMPUs can also respond to the solution (such as solvent) by a mechanism in which the solution molecule has a plasticizing effect on polymeric materials, thus increasing the flexibility of the macromolecule chains of the SMPU (Lv et al., 2008a). These two effects reduce the transition temperature of materials until shape recovery occurs (Lv et al., 2008b). There is an interaction between the polymeric macromolecule and the micromolecule of absorbed solution, and the hydrogen bonding enlarges the flexibility of polymeric chains. In brief, water, moisture, and solution-driven SMP provide alternative triggering approaches for SMEs, and so thermo-heating becomes unnecessary (Leng and Du, 2010).

9.3.5 Light triggering

Visible or infrared (IR) light-induced SME in SMPUs can be realized by incorporating reversible photoreactive molecule switches into the SMPUs (Jiang et al., 2006); for example, cinnamic acid or cinnamylidene acetic acid moieties (Lendlein et al., 2005). Upon irradiation with light, a (2+2) cycloaddition reaction occurs between two of these light-sensitive moieties, and in sequence, a cyclobutane-ring and in this way covalent cross-links form. Irradiation with a different wavelength results in cleavage of the newly formed bonds, which causes the light induced actuation effects.

Doping with 6 wt% chemical functionalized multi-walled carbon nanotubes by grafting dodecylamine chains, the photosensitivity of oxotitanium phthalocyanine (TiOPc) is fivefold higher than that of un-doped TiOPc when exposed to 570 nm wavelength (Huang et al., 2012). The idea of resonant absorption of light by nanoparticles has been applied to other systems for biomedical applications, such as drug release. The resonant frequency could shift from deep UV-light to near IR-light; smaller nanoparticles can absorb shorter wavelength light, whereas larger nanoparticles can absorb longer wavelength light (Huang et al., 2012). Au–Au_2S nanoparticles of ~20 nm consisting of Au_2S dielectric core encapsulated by a thin gold shell are reported to have absorption peak near-IR light and demonstrated a controlled drug release (Ren and Chow, 2003). The light absorption efficiency is strongly dependent on the size, shape, and concentration of the nanoparticles.

Irradiation using infrared light with wide emission spectra causes unique heating effect to the SMPU, which can be noncontact. The capability of absorbing infrared light is determined by molecule (or atom) constitution of materials, as infrared light is absorbed in the form of molecule (or atom) resonance vibration (Leng and Du, 2010; Huang et al., 2012). SMP/CB nanocomposites have showed strong (above 6%) continuum absorption in the range from 400 to 4000 cm^{-1} (Leng and Du, 2010). The existence of CB particles increases the capability to absorb infrared light for the SMP/CB composite remarkably (Leng and Du, 2010). When SMP and SMP/CB nanocomposites are exposed to infrared light, most of the emitted energy is transmitted by the SMP, which is semi-transparent, whereas most of the emitted infrared light is absorbed by the CB, since it is black and opaque, thus causing the heating effect (Leng and Du, 2010; Huang et al., 2012).

9.4 Medical applications of SMPU

PU-based SMPs have excellent biocompatibility, verified from standard cytotoxicity and mutagenicity tests (Gall et al., 2004; Small et al., 2009). The T_g of the SMPUs can be tailored for shape restoration/self-deployment of various clinical devices. Various shape-memory stimuli methods other than heat, such as alternating magnetic field or light, have broadened their applications substantially and extended their applications to noncontact operations (Huang et al., 2012).

Because of their good biocompatibility, there are many potential medical applications using the SMPUs (Fare et al., 2005; Sokolowski et al., 2007; Metcalfe et al., 2003). Key examples proposed for medical applications include:

- Thermoset SMPU actuators for treating ischemic stroke (Metzger et al., 2002)
- SMP microfluidic reservoirs (Gall et al., 2004)
- Intravascular thrombectomy to remove blood clots; infrared diode laser activated (Metzger et al., 2005)
- Thrombus removal activated by laser light (Small et al., 2005)
- Self-deployable SMP neuronal electrodes (Sharp et al., 2006)
- Vascular stent deployed *in vitro* by laser heating (Baer et al., 2007)
- SMP dialysis needle adapters for reducing hemodynamic stress in arteriovenous grafts (Ortega et al., 2007)
- Deployable biomedical devices for minimally invasive surgery (MIS) (Baer et al., 2007)
- SMPUs in cardiovascular implants (Sokolowski et al., 2007; Jung et al., 2010a,b)
- SMPs for bondages (Ahmad et al., 2012a,b,c)
- SMPs for ocular implants (Huang et al., 2012)
- SMPs for cell manipulation (Huang et al., 2012)

MIS is regarded as one of the most important achievements in modern medicine. The benefits compared to traditional methods include reduced operative trauma, fewer wound complications, shorter hospital stays, and accelerated recoveries (Huang et al., 2012). However, MIS is more technically demanding than conventional surgery because the surgical intervention is executed remotely via two-dimensional imaging of the operative field. As a result, a surgeon faces the loss of tactile feedback, restricted maneuverability, and less efficient control of major bleeding. Shape-memory materials provide good solutions to many problems in the MIS arena (Yahia, 2000; Yoneyama and Miyazaki, 2009; Huang et al., 2012). Stainless steel and shape-memory alloys have been the dominant materials for these applications; however, there are several drawbacks associated with the use of metallic stents: stiffness, compliance mismatch with the arterial wall, and the high cost of fabrication (Miyazaki et al., 2009). Therefore, SMPs, especially SMPUs, have more potential applications to replace the SMAs.

9.4.1 Sutures

A challenge in endoscopic surgery is to tie a knot with instruments and sutures to close an incision or open lumen, and sutures are commonly used during medical operations. MIS procedures generally allow only limited space for tying knots to secure sutures in place, and surgeons must tie knots remotely through very small holes. SMP has been applied in wound closure, and the suture can be applied loosely in its temporary shape under elongated stress (Huang et al., 2012). When the temperature is raised above T_g, the suture will shrink and then tighten the knot, in which case it will apply an optimum force. Since its maximum recovery stress is safe for human body tissues, damage caused by over-tightening is no longer a serious issue. Figure 9.11 reveals that upon

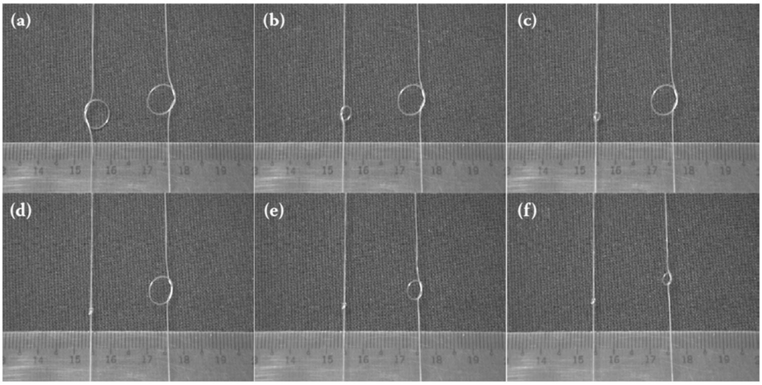

Figure 9.11 Self-tightening of two knots of SMP wires (MM3520) by immersion in room temperature water. The left piece was pre-immersed in water to reduce its T_g (Sun and Huang, 2010b).

immersion into room temperature water (about 22 °C), a polyurethane SMP knot tightens gradually (Sun and Huang, 2010a,b; Huang et al., 2012). Similarly, without heating, a knot can self-unravel and a suture can automatically tighten upon immersion into room temperature water. The sutures can also be biodegradable and show gradual mass loss during degradation (Lendlein and Kelch, 2005). For example, the hydrolyzable ester bonds are introduced into the polymers so that they would cleave under physiological conditions (Behl and Lendlein, 2007). If the SMP is biodegradable, sutures will self-degrade and disappear after time and even in a controllable manner (Lendlein and Kelch, 2005).

9.4.2 Stents

Vascular stents are small tubular scaffolds widely used in the treatment of arterial stenosis (narrowing of the vessel) to prevent acute vessel closure and late restenosis in a variety of vessels such as coronary arteries (Chen et al., 2007a, 2009). The increased flexibility, compliance, and relatively simple drug-embedding capability of SMPUs could overcome the problems encountered with current metallic vascular stents (Baer et al., 2007); for example, braided stents (Kim et al., 2010), solid-tube stents (Wache et al., 2003; Chen et al., 2007a,b; Yakacki et al., 2007), and even foam stents (Sokolowski et al., 2007). Other recent developments include drug-eluting stents and biodegradable stents (Chen et al., 2009; Wischke et al., 2010; Jung et al., 2010a,b; Wischke and Lendlein, 2010). The triggering mechanisms for the stents can be Joule heating or local laser heating (Maitland et al., 2002; Metzger et al., 2005; Baer et al., 2007; Huang et al., 2010a,b, 2012; Sun and Huang, 2010a,b).

Wache et al. (2003) conducted a feasibility study and a preliminary development on a polymer vascular stent with SMPs as a drug-delivery system. The use of the SMP stent

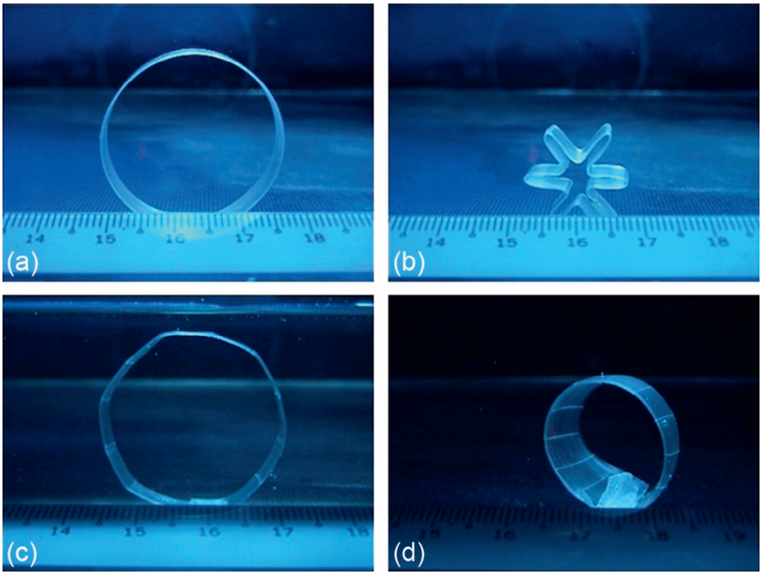

Figure 9.12 Retraction of a PU SMP stent in water. (a) After pre-stretching; (b) after folding; (c) after deployment in water; (d) after retraction in water.
Reproduced with permission from Yang et al. (2006).

as a drug-delivery system leads to significant reduction of restenosis and thrombosis. In bladder and prostate cancer treatments, retractable stents are preferred, but current conventional methods are mechanical dilations, endoscopic incision, or laser vaporization. Their success rates are low, and patients must undergo repeated treatments. A removable stent is a better option because it does not require a highly specialized reconstructive bladder neck repair procedure and is replaced annually. A retractable stents have been proposed to utilize the thermo- and moisture-responsive qualities of SMPUs (Huang et al., 2007). As shown in Figure 9.12, a SMP thin-wall tube was pre-expanded at high temperatures and then cooled back to room temperature (Yang et al., 2006). Subsequently, it was mechanically deformed into a star shape. After immersion into room temperature water, it mechanically expanded back into its circular shape. Since this SMP is also moisture-responsive, it shrinks after a time. As its diameter reduces, the stent can be easily removed (Huang et al., 2010a,b, 2012).

9.4.3 Cell and drug manipulation

Targeted drug release to specified cells at molecular level is currently an attractive topic in medical research (Han et al., 2010; Hartl and Hayer-Hartl, 2009). The thermo/moisture-responsiveness in polyurethane SMP sheds light on the possibility of realizing micro/nanodevices for surgery/operation at the cell level. As illustrated in Figure 9.13 (Sun and Huang, 2010b), a micro vehicle made of SMP is stretched and then inserted into a living cell. Upon absorbing moisture inside the cell, the

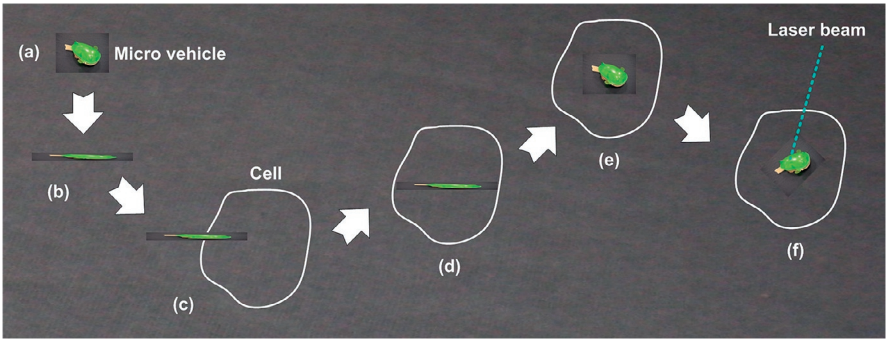

Figure 9.13 Delivery of a micro vehicle into a living cell for inside operation under a laser beam (illustration). (a) The original shape of a micro vehicle; (b) the shape of vehicle after reshaping; (c) inserting the deformed vehicle into a cell; (d) the vehicle fully inside the cell; (e) shape recovery of the vehicle; (f) in operation of the vehicle powered by a laser beam from outside. Reproduced from Sun and Huang (2010b).

SMP recovers its original shape. As the recovery strain in solid or porous SMPs is on an order of hundred percent, it becomes achievable to make cell- or sub-cell-sized machines using the thermo/moisture-responsive SMP and then deliver the machines into living cells for operation controlled by an outside laser beam (Johnson et al., 2007; Huang et al., 2010b).

9.4.4 Bandages

A venous leg ulcer is a common illness in developed countries (Fletcher et al., 1997). In this disease, the lower leg deteriorates because of reduced physical activity and poor blood circulation; the illness often affects the elderly. For patients with venous disease, application of gradient external compression can help minimize or reverse vascular change by forcing blood from the interstitial spaces back into the vascular and lymphatic compartments, hence leading to effective treatment (Ahmad et al., 2012c). Although there are various types of commercial bandages available for venous ulcer treatment, most have good elasticity but produce low compression forces.

Because pre-stretched thermal-responsive SMP strips will generate various shrinking forces upon heat stimulation, bandages made up of a number of SMP strips may generate distributed pressure and can be used for venous leg treatment (Ahmad et al., 2012a,b,c). An SMP actuator-based bandage has been proposed by Ahmad et al. (2012a,b,c) for leg ulcer treatments, as shown in Figure 9.14; they are made of a number of SMP strips with different strains with gradient pressure distribution. SMPUs have a suitable transition temperature range of 40–50 °C, have a low recovery stress (0.05–0.1 MPa), and are flexible. Therefore, these SMPUs are potentially useful in the proposed bandages. Thermal-responsive SMP strips are attached to fabrics that will be part of the underlay padding of the bandage, and the SMP strips are pre-stretched to fixed lengths or strains. In its fully developed form, the SMP bandage can be wrapped on the venous leg and held in position by Velcro fasteners or other similar means.

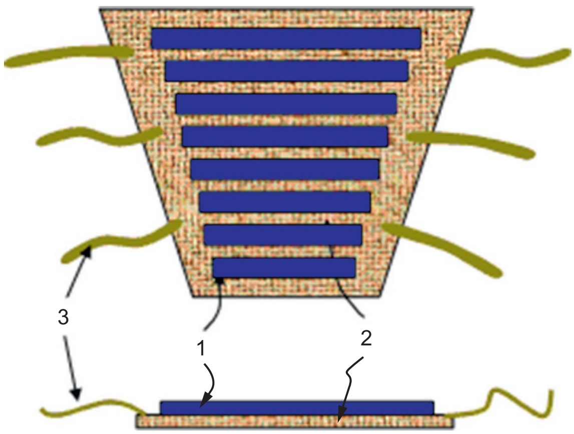

Figure 9.14 Design of the proposed SMP bandages, which can be applied/removed from a limb like a normal bandage once activated. 1, SMP strips; 2, Fabric; 3, Fasteners.

Upon application of an external heat using a normal hair dryer or a hot towel, the SMP stripes will shrink and partially return to their original shapes, providing a predefined force or pressure distribution acting on the venous leg for treatment. If the pressure drops during use, pressure readjustment can be easily achieved by using a hair dryer or a hot towel to warm up the SMP bandage, locally or as a whole. This can be done by the patient at home; without the need for a trained nurse/doctor, treatment is significantly simplified (Ahmad et al., 2012a,b,c).

9.4.5 *Other applications*

PU-based SMPs have potential as artificial muscles for a prosthesis if they can develop relatively large forces (1–3 MPa) and are able to shrink or elongate (Yahia, 2000; Metzger et al., 2002, 2005). SMP materials can be used to manufacture catheters that remain stiff externally for accurate manipulation by the physician, but become softer and more comfortable inside the human body. With a soft catheter, there will be fewer arterial wall injuries than with the conventional rigid catheter. They will also be easier to manipulate and apply into tortuous vessels.

A blood clot may cause an ischemic stroke, depriving the brain of oxygen and often resulting in permanent disability. As an alternative to conventional clot-dissolving drug treatment, a laser-activated device for the mechanical removal of blood clots has been proposed (Small et al., 2005). The deformed SMPU straight rods could be inserted by MIS into the vascular occlusion. The microactuator, which is mounted on the end of an optical fiber, is then transformed into its pre-deformed corkscrew shape by laser heating. Once deployed into the corkscrew shape, the microactuator is retracted from the captured thrombus, enabling the mechanical removal of the thrombus (Small et al., 2009).

Maitland et al. (2002) reported thermally activated SMP-based mechanical clot extraction devices to treat ischemic stroke. These devices were designed to be delivered through a catheter and penetrate the clot in a narrow form and then actuate into a clot-grabbing form for extraction. After doping the SMP with dye, laser-absorbing photothermal actuation of corkscrew-shaped and umbrella-shaped devices have been demonstrated, which can be actuated using a diode laser operating at a wavelength of 810 nm into the SMP device. Metzger et al. (2002, 2005) further demonstrated that the SMP corkscrew device could hold a blood clot against vascular physiological forces.

Mitral valve insufficiency occurs when the mitral valve does not close properly, resulting in the regurgitation of blood from the left ventricle to the left atrium (flow reversal). Valve repair, as opposed to replacement, is the preferred method of treatment; SMPU would be a good candidate (Enriquez-Sarano et al., 1995). SMPs can also be applied for minimally invasive tissue engineering. Tissues can be grown on SMP scaffolds and potentially delivered into the body using minimally invasive techniques and implanted to initiate repair or reconstruction of tissues or organs (Small et al., 2009). Biodegradable SMPs could be applied in pharyngeal mucosa reconstruction, bone regeneration, and organ repair (Small et al., 2009).

9.5 Summary and future trends

PU-based SMPs are smart materials with the unique characteristic of remembering their original shapes upon stimulation. They have been widely used in engineering, space exploration, and particularly in medical devices. Although SMPUs possess low mechanical strength and recovery stress compared to shape-memory alloys, their unique properties, such as high-shape recovery ratio, low recover stress, and flexibility, make them significant for various applications. SMPUs have many excellent properties: they are easy to manufacture, have a strong resistance to organic solvents and aqueous solutions, offer good, long-term stability against sunlight exposure, and have excellent and consistent elastic properties as well as biocompatibility. The multiple-responsive shape-memory feature of SMPUs further enables them to be used as a potential candidate for many biomedical devices, in particular MIS.

Properties of SMPUs can be tailored by varying the molecular weight of polyol, hard segment content, chain extender, or even moisture. Low recovery stress, modulus, and stiffness in SMPs are the main obstacles for their wide application. Incorporation of metals, nanofillers, clays, and tubes into PU matrices not only enhance the mechanical properties and recovery stress of SMPs, but also produce multifunctional composites. Shape recovery of SMPUs is normally a thermally induced process; however, they can also be triggered optically, electrically, magnetically, or electromagnetically, or by water or moisture, by adding various functional fillers. Various shape-memory stimuli methods other than heat, such as alternating magnetic field or light, have broadened their applications substantially and extended their applications to noncontact operations. The SMPUs have been proposed for many biomedical applications, including thermoset SMPU actuators for treating ischemic stroke, thrombus removal activated by laser light, self-deployable SMP neuronal electrodes, vascular stent, suture in microsurgery, ocular implants, bondages, cell manipulation, and cell therapy.

References

Ahir, S.V., Terentjev, E.M., 2005. Photomechanical actuation in polymer–nanotube composites. Nat. Mater. 4, 491–495.

Ahir, S.V., Tajbakhsh, A.R., Terentjev, E.M., 2006. Self-assembled shape-memory fibre of triblock liquid–crystal polymers. Adv. Funct. Mater. 16, 556–560.

Ahmad, M., Luo, J.K., Xu, B., Purnawali, H., King, P.J., Chalker, P., Fu, Y.Q., Huang, W.M., Miraftab, M., 2011. Synthesis and characterization of polyurethane-based shape memory polymers for tailored T_g around body temperature for medical applications. Macromol. Chem. Phys. 202, 592–602.

Ahmad, M., Luo, J.K., Miraftab, M., 2012a. Feasibility study of polyurethane shape-memory polymer actuators for pressure bandage application. Sci. Technol. Adv. Mater. 13, 015006.

Ahmad, M., Xu, B., Purnawali, H., Fu, Y.Q., Huang, W.M., Miraftab, M., Luo, J.K., 2012b. High performance shape memory polyurethane synthesized with high molecular weight polyols as soft segment. Appl. Sci. 2, 535–548.

Ahmad, M., Luo, J.K., Purnawali, H., Huang, W.M., King, P.J., Chalker, P.R., Miraftab, M., 2012c. Making shape memory polymers reprocessable and reusable by a simple chemical method. J. Mater. Chem. 20 (2012), 3442–3448.

Baer, G.M., Wilson, T.S., Benett, W.J., et al., 2007. Fabrication and in vitro deployment of a laser activated shape memory polymer vascular stent. BioMed. Eng. Online 6, 43.

Bassi, M., Tonelli, C., Di, A.M., 2003. Glass transition behavior of a microphase segregated polyurethane based on PFPE and IPDI. A calorimetric study. Macromolecules 36, 8015.

Behl, M., Lendlein, A., 2007. Shape-memory polymers. Mater. Today 10, 20–28.

Behl, M., Lendlein, A., 2010. Triple-shape polymers. J. Mater. Chem. 20, 3335–3345.

Bellin, I., Kelch, S., Langer, R., et al., 2006. Polymeric triple-shape materials. Proc. Natl. Acad. Sci. U. S. A. 103, 18043–18047.

Bellin, I., Kelch, S., Lendlein, A., 2007. Dual-shape properties of triple-shape polymer networks with crystallizable network segments and grafted side chains. J. Mater. Chem. 17, 2885–2891.

Bryning, M.B., Islam, M.F., Kikkawa, J.M., Yodh, A.G., 2005. Very low conductivity threshold in bulk isotropic single-walled carbon nanotube–epoxy composites. Adv. Mater. 17, 1186–1191.

Buckley, P.R., McKinley, G.H., Wilson, T.S., Small, W., et al., 2006. Inductively heated shape memory polymer for the magnetic actuation of medical devices. IEEE Trans. Biomed. Eng. 53, 2075–2083.

Cao, F., Jana, S.C., 2007. Nanoclay-tethered shape memory polyurethane nanocomposites. Polymer 48, 3790–3800.

Chen, S.J., Cao, Q., Jing, B., Cai, Y.L., Liu, P.S., Hu, J.L., 2006. Effect of microphase-separation promoters on the shape-memory behavior of polyurethane. J. Appl. Polym. Sci. 102, 5224.

Chen, M., Tsai, H., Chang, Y., et al., 2007a. Rapidly self-expandable polymeric stents with a shape-memory property. Biomacromolecules 8, 2274–2780.

Chen, S.J.J., Hu, L., Liu, Y.Q., Liem, H.M., Zhu, Y., Liu, Y.J., 2007b. Effect of SSL and HSC on morphology and properties of PHA based SMPU synthesized by bulk polymerization method. J. Polym. Sci. Pt. B-Polym. Phys. 45, 444–454.

Chen, M., Chang, Y., Liu, C., et al., 2009. The characteristics and *in vivo* suppression of neointimal formation with sirolimus-eluting polymeric stents. Biomaterials 30, 79–88.

Cho, J.W., Kim, J.W., Jung, Y.C., Goo, N.S., 2005. Electroactive shape-memory polyurethane composites incorporating carbon nanotubes. Macromol. Rapid Commun. 26, 412–416.

Choi, N.Y., Kelch, S., Lendlein, A., 2006. Synthesis, shape-memory functionality and hydrolytical degradation studies on polymer networks from poly(rac-lactide)-*b*-poly(propylene oxide)-*b*-poly(rac-lactide) dimethacrylates. Adv. Eng. Mater. 8, 439–445.
Chun, B.C., Cho, T.K., Chung, Y.C., 2006. Enhanced mechanical and shape memory properties of polyurethane block copolymers chain-extended by ethylene diamine. J. Eur. Polym. 42, 3367.
Ding, X.M., Hu, J.L., Tao, X.M., Hu, C.P., 2006. Preparation of temperature sensitive polyurethanes for smart textiles. J. Tex. Res. 76, 406.
El-Feninat, F., Laroche, G., Fiset, M., Mantovani, D., 2002. Shape memory materials for biomedical applications. Adv. Eng. Mater. 4, 91–104.
Enriquez-Sarano, M., Tajik, A.J., Bailey, K.R., Seward, J.B., 1993. Color flow imaging compared with quantitative Doppler assessment of severity of mitral regurgitation: influence of eccentricity of jet and mechanism of regurgitation. J. Am. Coll. Cardiol. 21, 1211–1219.
Fare, S., Valtulina, V., Petrini, P., Alessandrini, E., Pietrocola, G., Tanzi, M.C., Speziale, P., Visai, L., 2005. In vitro interaction of human fibroblasts and platelets with a shape-memory polyurethane. J. Biomed. Mater. Res. A 73A, 1–11.
Fletcher, A., Cullum, N., Sherdon, T.A., 1997. A systematic review of compression treatment for venous leg ulcers. J. Br. Med. 315, 576.
Gall, K., Mikulas, M., Munshi, N.A., Beavers, F., Tupper, M., 2000. Carbon fiber reinforced shape memory polymer composites. J. Intell. Materials Syst. Struct. 11, 877–886.
Gall, K., Kreiner, P., Turner, D., et al., 2004. Shape-memory polymer for microelectromechanical systems. J. Microelectromechanical Syst. 13, 472–483.
Goethals, E.J., Reyntjens, W., Lievens, S., 1998. Poly(vinyl ethers) as building blocks for new materials. Macromol. Symp. 132, 57–64.
Gunes, I.S., Jana, S.C., 2008. Shape memory polymers and their nanocomposites: a review of science and technology of new multifunctional materials. J. Nanosci. Nanotechnol. 8, 1616–1637.
Gunes, I.S., Cao, F., Jana, S.C., 2008. Evaluation of nanoparticulate fillers for development of shape memory polyurethane nanocomposites. Polymer 49, 2223–2234.
Gunes, I.S., Jimenez, G.A., Jana, S.C., 2009. Carbonaceous fillers for shape memory actuation of polyurethane composites by resistive heating. Carbon 47, 981–997.
Han, D., Pal, S., Liu, Y., et al., 2010. Folding and cutting DNA into reconfigurable topological nanostructures. Nat. Nanotechnol. 5, 712–717.
Hartl, F.U., Hayer-Hartl, M., 2009. Converging concepts of protein folding *in vitro* and *in vivo*. Nat. Struct. Mol. Biol. 16, 574–581.
Hayashi, S., 1990. Technical report on preliminary investigation of shape memory polymers. Mitsubishi Heavy Industries, Research and Development Center, Nagoya, Japan.
Hu, J.L., Zeng, Y.M., Yan, H.J., 2003. Influence of processing conditions on the microstructure and properties of shape memory polyurethane membranes. Text. Res. J. 73, 172.
Huang, W.M., 2010. Thermo-moisture responsive polyurethane shape memory polymer for biomedical devices. Open Med. Dev. J. 2, 11–19.
Huang, W.M., Yang, B., An, L., et al., 2005. Water-driven programmable polyurethane shape memory polymer: demonstration and mechanism. Appl. Phys. Lett. 86, 114105.
Huang, W.M., Lee, C.W., Teo, H.P., 2006. Thermomechanical behavior of a polyurethane shape memory polymer foam. J. Intell. Mater. Syst. Struct. 17, 753–760.
Huang, W.M., Yang, B., Liu, N., Phee, S.J., 2007. Water-responsive programmable shape memory polymer devices. Int. Conf. Smart Mater. Nanotechnol. Eng. 6423, 64231–64237.
Huang, W.M., Yang, B., Zhao, Y., Ding, Z., 2010a. Thermo-moisture responsive polyurethane shape-memory polymer and composites: a review. J. Mater. Chem. 20, 3367–3381.
Huang, W.M., Ding, Z., Wang, C.C., et al., 2010b. Shape memory materials. Mater. Today 13, 44–51.

Huang, W.M., Yang, B., Fu, Y.Q., 2012. Polyurethane Shape Memory Polymers. CRC Press, Boca Raton, FL, USA, 33487-2742.
Jeong, H.M., Lee, S.Y., Kim, B.K., 2000. Shape memory polyurethane containing amorphous reversible phase. J. Mater. Sci. 35, 1579–1583.
Jiang, H.Y., Kelch, S., Lendlein, A., 2006. Polymers move in response to light. Adv. Mater. 18, 1471–1475.
Johnson, C.P., Tang, H., Carag, C., et al., 2007. Forced unfolding of protein within cells. Science 317, 663–666.
Jung, Y.C., Cho, J.W., 2010. Application of shape memory polyurethane in orthodontic. J. Mater. Sci. Mater. Med. 21, 2881–2886.
Jung, F., Wischke, C., Lendlein, A., 2010a. Degradable, multifunctional cardiovascular implants: challenges and hurdles. MRS Bull. 35, 607–613.
Jung, Y.C., Yoo, H.J., Kim, Y.A., Cho, J.W., Endo, M., 2010b. Electroactive shape memory performance of polyurethane composite having homogeneously dispersed and covalently cross-linked carbon nanotubes. Carbon 48, 1598–1603.
Kim, B.K., Lee, S.Y., Xu, M., 1996. Polyurethanes having shape memory effect. Polymer 37, 5781–5793.
Kim, J.H., Kang, T.J., Yu, W., 2010. Simulation of mechanical behavior of temperature-responsive braided stents made of shape memory polyurethanes. J. Biomech. 43, 632–643.
Koerner, H., Price, G., Pearce, N.A., Alexander, M., Vaia, R., 2004. Remotely actuated polymer nanocomposites—stress-recovery of carbon-nanotube-filled thermoplastic elastomers. Nat. Mater. 3, 115–120.
Kumar, U.N., Kratz, K., Wagermaier, W., et al., 2010. Non-contact actuation of triple-shape effect in multiphase polymer network nanocomposites in alternating magnetic field. J. Mater. Chem. 20, 3404–3415.
Lee, B.S., Chun, B.C., Chung, Y.C., Sul, K.I., Cho, J.W., 2001. Structure and thermomechanical properties of polyurethane block copolymers with shape memory effect. Macromolecules 34, 6431.
Lee, S.H., Kim, J.W., Kim, B.K., 2004. Shape memory polyurethanes having crosslinks in soft and hard segments. Smart Mater. Struct. 13, 1345–1350.
Lendlein, A., Kelch, S., 2002. Shape-memory polymers. Angew. Chem. Int. Ed. 41, 2034–2057.
Lendlein, A., Kelch, S., 2005. Degradable, multifunctional polymeric biomaterials with shape-memory. In: Van der Biest, O., et al. (Ed.), In: Functionally Graded Materials VIII, vol. 219. Technology Transition Publications, Leuven, Belgium, pp. 492–493.
Lendlein, A., Jiang, H., Junger, O., Langer, R., 2005. Light-induced shape-memory polymers. Nature 434, 879–882.
Leng, J.S., Du, S.Y., 2010. Shape-Memory Polymers and Multifunctional Composites. CRC Press, Boca Raton, FL.
Leng, J., Lv, H., Liu, Y., Du, S., 2007. Electroactivate shape-memory polymer filled with nano-carbon particles and short carbon fibers. Appl. Phys. Lett. 91, 144105.
Leng, J.S., Huang, W.M., Lan, X., Liu, Y.J., Liu, N., Phee, S.Y., Du, S.Y., 2008a. Significantly reducing electrical resistivity by forming conductive Ni chains in a polyurethane shape-memory polymer/carbon-black composite. Appl. Phys. Lett. 92, 204101.
Leng, J.S., Lan, X., Huang, W.M., Liu, Y.J., Liu, N., Phee, S.Y., Du, S.Y., et al., 2008b. Electrical conductivity of shape memory polymer embedded with micro Ni chains. Appl. Phys. Lett. 92, 014104.
Liang, C., Rogers, C.A., Malafeew, E., 1997. Investigation of shape memory polymers and their hybrid composites. J. Intel. Mat. Syst. Str. 8, 380–386.

Liu, G.Q., Ding, X.B., Cao, Y.P., et al., 2005. Novel shape-memory polymer with two transition temperatures. Macromol. Rapid Commun. 26, 649–652.
Liu, Y., Lv, H., Lan, X., Leng, J., Du, S., 2009. Review of electro-active shape-memory polymer composite. Compos. Sci. Technol. 69, 2064.
Lv, H.B., Leng, J.S., Liu, Y.J., Du, S.Y., 2008a. Shape-memory polymer in response to solution. Adv. Eng. Mater. 10, 592–595.
Lv, H.B., Liu, Y.J., Zhang, D., Leng, J.S., Du, S., 2008b. Solution-responsive shape-memory polymer driven by forming hydrogen bonding. Adv. Mater. Res. 47–50, 258–261.
Ma, Z.L., Zhao, W.G., Liu, Y.F., Shi, J.R., 1997. Intumescent polyurethane coatings with reduced flammability based on spirocyclic phosphate-containing polyols. J. Appl. Polym. Sci. 66, 471–475.
Maitland, D.J., Metzger, M.F., Schumann, D., et al., 2002. Photothermal properties of shape memory polymer micro-actuators for treating stroke. Lasers Surg. Med. 30, 1–11.
Meng, Q.H., Hu, J.L., 2009. A review of shape memory polymer composites and blends. Composites A 40, 1661.
Merlin, M., 2008. Using NiTi shape memory alloy wires for the geometry active control in a cooling fan. Adv. Geomater. Struct. 1, 51–61.
Merline, J.D.C., Nair, P.R., Gouri, C., Bandyopadhyay, G.G., Ninan, K.N., 2008. Polyether polyurethanes: synthesis, characterization, and thermoresponsive shape memory properties. J. Appl. Polym. Sci. 107, 4082–4092.
Metcalfe, A., Desfaits, A.C., Salazkin, I., Yahia, L., Sokolowski, W.M., Raymond, J., 2003. Cold hibernated elastic memory foams for endovascular interventions. Biomaterials 24, 491–497.
Metzger, M.F., Wilson, T.S., Schumann, D., et al., 2002. Mechanical properties of mechanical actuator for treating ischemic stroke. Biomed. Microdevices 4, 89–96.
Metzger, M.F., Wilson, T.S., Maitland, D.J., 2005. Laser-activated shape memory polymer microactuator for thrombus removal following ischemic stroke: preliminary *in vitro* analysis. IEEE J. Selected Top. Quantum Electron. 11, 892–900.
Miaudet, P., Derre, A., Maugey, M., et al., 2007. Shape and temperature memory of nanocomposites with broadened glass transition. Science 318, 1294–1296.
Miyazaki, S., Fu, Y.Q., Huang, W.M., 2009. Thin Film Shape Memory Alloys: Fundamentals and Device Applications. Cambridge University Press, Cambridge.
Monkman, G.J., 2000a. Advances in shape memory polymer actuation. Mech. Mater. 10, 489.
Monkman, G.J., 2000b. Advances in shape memory actuation. Mechatronics 10, 489–498.
Ortega, J., Maitland, D.J., Wilson, T.S., Tsai, W., Savas, O., Saloner, D., 2007. Vascular dynamics of a shape memory polymer foam aneurysm treatment technique. Annu. Biomed. Eng. 35, 1870–1884.
Paik, I.H., Goo, N.S., Jung, Y.C., Cho, J.W., 2006. Development and application of conducting shape memory polyurethane actuators. Smart Mater. Struct. 15, 1476–1482.
Pretsch, T., 2010. Triple-shape properties of a thermoresponsive poly(ester urethane). Smart Mater. Struct. 19, 015006.
Razzaq, M.Y., Anhalt, M., Frormann, L., Weidenfeller, B., 2007a. Thermal, electrical and magnetic studies of magnetite filled polyurethane shape memory polymers. Mater. Sci. Eng. A 444, 227–235.
Razzaq, M.Y., Anhalt, M., Frormann, L., Weidenfeller, B., 2007b. Mechanical spectroscopy of magnetite filled polyurethane shape memory polymers. Mater. Sci. Eng. A 471, 57–62.
Ren, L., Chow, G.M., 2003. Synthesis of NIR-sensitive Au–Au_2S nanocolloids for drug delivery. Mat. Sci. Eng. C 23, 113.
Sahoo, N.G., Jung, Y.C., Goo, N.S., Cho, J.W., 2005. Conducting shape memory polyurethane-polypyrrole composites for an electroactive actuator. Macromol. Mater. Eng. 290, 1049–1055.

Sahoo, N.G., Rana, S., Cho, J.W., Li, L., Chan, S.H., 2010. Polymer nanocomposites based on functionalized carbon nanotubes. Prog. Polym. Sci. 35, 837–867.

Sandler, J.K.W., Kirk, J.E., Kinloch, I.A., Shaffer, M.S.P., Windle, A.H., 2003. Ultra-low electrical percolation threshold in carbon-nanotube-epoxy composites. Polymer 44, 5893–5899.

Schmidt, A.M., 2006. Electromagnetic activation of shape memory polymer networks containing magnetic nanoparticles. Macromol. Rapid Commun. 27, 1168–1172.

Sharp, A.A., Panchawagh, H.V., Ortega, A., et al., 2006. Toward a self-deploying shape memory polymer neuronal electrode. J. Neural Eng. 3, L23–L30.

Small, W., Wilson, T.S., Benett, W.J., Loge, J.M., Maitland, D.J., 2005. Laser activated shape memory polymer intravascular thrombectomy device. Opt. Express 13, 8204–8213.

Small IV, W., Singhal, P., Wilson, T.S., Maitland, D.J., 2010. Biomedical applications of thermally activated shape memory polymers. J. Mater. Chem. 20 (18), 3356–3366.

Sokolowski, W., Metcalfe, A., Hayashi, S., et al., 2007. Medical applications of shape memory polymers. Biomed. Mater. 2, S23–S27.

Spinks, G.M., Mottaghitalab, V., Bahrami-Saniani, M., Whitten, P.G., Wallace, G.G., 2006. Carbon-nanotube-reinforced polyaniline fibers for high-strength artificial muscles. Adv. Mater. 18, 637.

Sun, L., Huang, W.M., 2010a. Mechanisms of the multi-shape memory effect and temperature memory effect in shape memory polymers. Soft Matter 6, 4403–4406.

Sun, L., Huang, W.M., 2010b. Thermo/moisture responsive shape-memory polymer for possible surgery/operation inside living cells in future. Mater. Design 31, 2684–2689.

Sun, L., Huang, W.M., Cheah, J.Y., 2010. The temperature memory effect and the influence of thermo-mechanical cycling in shape memory alloys. Smart Mater. Struct. 19, 055005.

Szycher, M., 1999. Szycher's Handbook of Polyurethanes. CRC Press, Boca Raton.

Tobushi, H., Hayashi, S., Kojima, S., 1992. Mechanical properties of shape memory polymer of polyurethane series: basic characteristics of stress-strain-temperature relationship. JSME Int. J. Ser. 1 (35), 296–302.

Tobushi, H., Hara, H., Yamada, E., et al., 1996. Thermomechanical properties in a thin film of shape memory polymer of polyurethane series. Smart Mater. Struct. 5, 483–491.

Tobushi, H., Okumura, K., Hayashi, S., Ito, N., 2001. Thermomechanical constitutive model of shape memory polymer. Mech. Mater. 33, 545–554.

Wache, H.M., Tartakowska, D.J., Hentrich, A., et al., 2003. Development of polymer stent with shape memory effect as a drug delivery system. J. Mater. Sci. Mater. Med. 14, 109–112.

Wei, Z.G., Sandstrorӧm, R., Miyazaki, S., 1998. Shape-memory materials and hybrid composites for smart systems: Part I Shape-memory materials. J. Mater. Sci. 33, 3743–3762.

Weigel, T., Mohr, R., Lendlein, A., 2009. Investigation of parameters to achieve temperatures required to initiate the shape-memory effect of magnetic nanocomposites by inductive heating. Smart Mater. Struct. 18, 025011.

Wischke, C., Lendlein, A., 2010. Shape-memory polymers as drug carriers - a multifunctional system. Pharm. Res. 27, 527–529.

Wischke, C., Beffe, A.T., Lendlein, A., 2010. Controlled drug release from biodegradable shape-memory polymers. Adv. Polym. Sci. 226, 177–205.

Xie, T., 2010. Tunable polymer multi-shape memory effect. Nature 464, 267–270.

Xie, T., Xiao, X.C., Cheng, Y.T., 2009. Revealing triple-shape memory effect by polymer bilayers. Macromol. Rapid Commun. 30, 1823–1827.

Xu, B., Huang, W.M., Pei, Y.T., et al., 2009. Mechanical properties of attapulgite clay-reinforced polyurethane shape memory nanocomposites. Eur. Polym. J. 45, 1904–1911.

Xu, B.Y.Q.Fu., Ahmad, M., Luo, J.K., Huang, W.M., Kraft, A., Reuben, R., Pei, Y.T., Chen, Z. G., Th, J., De Hosson, M., 2010. Thermo-mechanical properties of polystyrene-based shape memory nanocomposites. J. Mater. Chem. 20, 3442–3448.
Yahia, L., 2000. Shape memory implants. In: Yakacki, C.M., Shandas, R., Lanning, C., et al. (Eds.), Unconstrained Recovery Characterization. Springer, Heidelberg.
Yakacki, C.M., Shandas, R., Lanning, C., Rech, B., Eckstein, A., Gall, K., 2007. Unconstrained recovery characterization of shape-memory polymer networks for cardiovascular applications. Biomaterials 28, 2255–2263.
Yakacki, C.M., Satarkar, N.S., Gall, K., Likos, R., Hilt, J.Z., 2009. Shape-memory polymer networks with Fe_3O_4 nanoparticles for remote activation. J. Appl. Polym. Sci. 112, 3166–3176.
Yang, B., 2007, Characterisation of polyurethane shape memory polymers. PhD Thesis, Nanyang Technological University, Singapore.
Yang, J.H., Chun, B.C., Chung, Y., Cho, J.H., 2003. Comparison of thermal/mechanical properties and shape memory effect of polyurethane block-copolymers with planar or bent shape of hard segment. Polymer 44, 3251.
Yang, B., Huang, W.M., Li, C., Lee, C.M., Li, L., 2004. On the effects of moisture in a polyurethane shape memory polymer. Smart Mater. Struct. 13, 191–195.
Yang, B., Huang, W.M., Li, C., Li, L., Chor, J.H., 2005. Qualitative separation of the effects of carbon nanopowder and moisture on the glass transition temperature of polyurethane shape memory polymer. Scr. Mater. 53, 105–107.
Yang, B., Huang, W.M., Li, C., Li, L., 2006. Effects of moisture on the thermomechanical properties of a polyurethane shape memory polymer. Polymer 47, 1348–1356.
Yang, F., Wornyo, E., Gall, K., King, W.P., 2007. Nanoscale indent formation in shape memory polymers using a heated probe tip. Nanotechnology. 18, 285302.
Yoneyama, T., Miyazaki, S., 2009. Shape Memory Alloys for Biomedical Applications. Woodhead Publishing Limited, Cambridge, UK.
Zhang, C.S., Ni, Q.Q., Fu, S.Y., Kurashiki, K., 2007. Electromagnetic interference shielding effect of nanocomposites with carbon nanotube and shape memory polymer. Compos. Sci. Technol. 67, 2973–2980.
Zhao, Y., Huang, W.M., Fu, Y.Q., 2011. Formation of micro/nano-scale wrinkling patterns atop shape memory polymers. J. Micromech. Microeng. 21, 067007.
Zhu, Y., Hu, J.L., Yeung, L.Y., Liu, Y., Ji, F.L., Yeung, K.W., 2006. Development of shape memory polyurethane fiber with complete shape recoverability. Smart Mater. Struct. 15, 1385–1394.
Zhuo, H.T., Hu, J.L., Chen, S.J., 2008. Electrospun polyurethane nanofibres having shape memory effect. Mater. Lett. 62, 2074–2076.
Zdrahala, R.J., Zdrahala, I.J., 1999. Biomedical applications of polyurethanes: a review of past promises, present realities, and a vibrant future. J. Biomater. Appl. 14, 67–90.